ERJ
Engineering Research Journal
Faculty of Engineering
Minoufiya University

FAILURE ANALYSIS OF STEEL ADHESIVE BONDED CONNECTIONS: EXPERIMENTAL AND NUMERICAL STUDIES

Saba, A. M. Seleem, M. H., Sharaky, I. A. and Sallam, H. E. M.

Materials Engineering Department, Zagazig University, Zagazig, EGYPT

ABSTRACT

Degradation of many steel structures is caused as a result of corrosion or fatigue. The methods of repair in theses cases are connecting steel plate to the damaged position by welding, bolting or adhesive bonding technique. In this paper, experimental and numerical programs were conducted to investigate the behavior of steel connections by adhesive bonding technique. The effects of the length of bonded plates, bonded plate ends geometry, main plate ends geometry and the presence of damage in the main plate were investigated. The stress concentration due to the fatigue or corrosion damage in the main plate is simulated as a double edge notch or a central hole. The connections were tested under tensile axial load. Ultimate load, load elongation behavior and modes of failure of the tested connections were recorded. All tested connections were simulated numerically using the general-purpose three dimensional (3D) finite element analysis (FEA) program ABAQUS to understand the debonding initiation and growth. All adhesive connections were failed due debonding when the stress in the main steel plates at the ends of the bonded plates reached the yield stress.

يتعرض هذا البحث بالدراسة المعملية والعددية لتطبيق أسلوب الربط باللصق على وصلات الصلب المعرضة لأحمال الشد. وقد تمت دراسة تأثير طول وشكل النهايات لألواح الربط على كفاءة الوصلة ونمط الانهيار في هذه الوصلات وتم أيضا دراسة تأثير وجود أماكن تركيز للاجهادات مثل الشروخ والفتحات الدائرية في ألواح الصلب المدعمة على سلوك هذه الألواح، وتمت الدراسة العددية باستخدام طريقة العناصر المحدودة ذات الأبعاد الثلاثية لمحاكاة ألواح الصلب المدعمة بلصق ألواح من نفس المادة وقورنت النتائج العددية بنظيراتها المعملية. وقد لوحظ أن جميع الوصلات الملصوقة تنفصل عندما يصل الإجهاد في اللوح الأساسي المربوط إلى مرحلة الخضوع والذي يبدأ في اللوح الأساسي عند نهاية ألواح الربط.

Keywords: Steel connections; Adhesive bonding; Bonded length; 3D Finite element.

1. INTRODUCTION

Recently, steel and wrought iron structures (mostly bridges) have been strengthened or repaired using adhesively-bonded carbon fiber laminates [1-3]. If the designer establishes adhesive joints, large stresses are present within it. The designer must find a way to accommodate them. One option is to seek a higher strength joint by using a different adhesive. However, this is rarely possible due to the greater demands on the quality of surface preparation prior to bonding. Alternatively, the designer can modify the geometry of the strengthening and adhesive close to the end of the plate to reduce the maximum adhesive stresses [4].

There is some lack of knowledge regarding how proper selection of materials for the different applications [5]. In adhesive bonding, the interfacial stress concentration (SC) at the plate ends have been known to be the most detrimental feature. This is due to the discontinuity caused by the abrupt termination of the plate. The governing parameters controlling SC at the edge of the adhesive bonded plates were investigated by Tounsi et al. [6]. Force transfer between the bonded and main plates takes place through bond at the interface between the two materials, which is influenced by several factors including bonded length, types of bonded plate and adhesive materials, surface preparation, thickness of adhesive and thickness of bonded plates [7-10]. Spew fillets and end tapers have been suggested for reducing the SC in the adhesive layer of retrofitted beams [11]. The main objective of the present work is to examine the applicability of adhesive bonding technique for bonding steel plates. The effects of length, ends configuration of bonded plates were investigated. The effect of the presence of SC sites in the main plate was also studied.

2. EXPERIMENTAL WORK

The experimental program was conducted in two groups to investigate the behavior of steel connections in the absence or presence of cracks or holes. All specimens were tested under axial tensile stress. The load elongation curve, ultimate loads and modes of failure of the tested connections were recorded.

2.1 Group I

In this group, a total of four double-lap shear connections (D, E, H and N) were tested. For the first three connections (D, E and H), the dimensions of the

main steel plate were 500 mm long, 60 mm wide and 4 mm thickness. The main steel plate was cut into two parts and then connected by two bonded steel plates having the same cross section dimensions of the main steel plate with different end configurations, square end (D), tapered end (E) and circular end (H) as shown in Fig. 1.

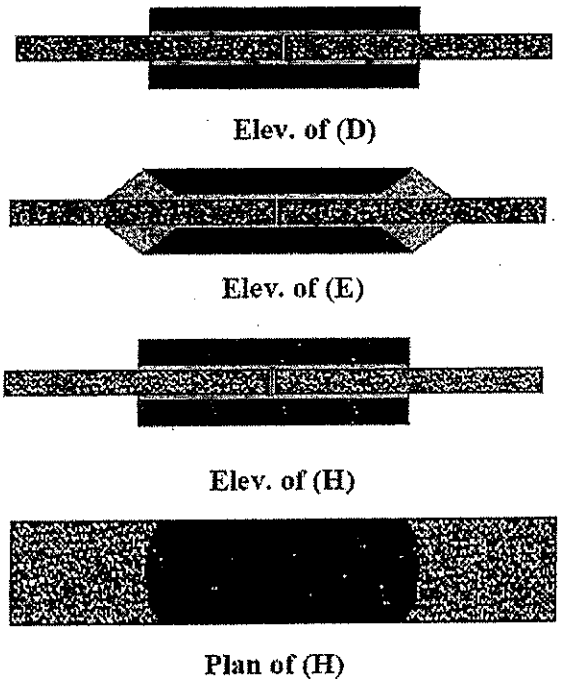

Fig.1. Configurations of connections tested in group I.

The length of the bonded steel plates used for the three connections (D, E and H) was 250 mm. The connection N was tested to study the effect of the length of the bonded steel plates. The dimensions of the main steel plate for this connection were 1000 mm long, 60 mm wide and 4 mm thickness. The main steel plate was cut into two equal parts. The ends of the main plate at the location of cut were square. The two parts of the main plate were connected by two bonded steel plates of 500 mm length and having the same cross section dimensions of the main steel plate.

2.1 Group II

This group was designed with the objective of studying the effect of the presence of damage such as double edge notch (DEN) or central hole (CH) on the performance of the adhesive connections. A total of seven plates, 500 mm long, 60 mm wide and 4 mm thickness were investigated. In the fist four plates, a DEN (15 mm depth and 1 mm radius) was created at the middle length of the steel plate. One of the four plates was tested as it is without any repair and denoted as U. The other three plates were strengthened using two bonded steel plates (each plate has a width of 15 mm) in each side, as shown in Fig. 2. The lengths of the bonded steel plates (l_{BP}) were 250 mm for configuration A, 200 mm for configuration B and 150 mm for configuration C. The thickness of the bonded steel plates was 4 mm.

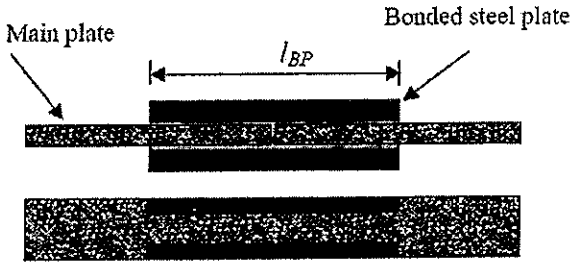

Fig.2. Configurations of connections A, B and C tested in group II.

The remaining three specimens (R, H_{30}, H_{30S}) were as follow: The dimensions of the main plates in the three connections were 1000 mm long, 60 mm wide and 4 mm thick. The plate R was tested as a reference without the application of any strengthening technique. In the second plate, H_{30}, a circular hole with 30 mm diameter was drilled in the specimen center, see Fig3a and tested without the application of any strengthening technique. The third specimen, H_{30S} was the same as H_{30} but strengthened with bonded steel plates 500 mm long, 30 mm width and 4 mm thick at the two sides of the main plate, see Fig.3b.

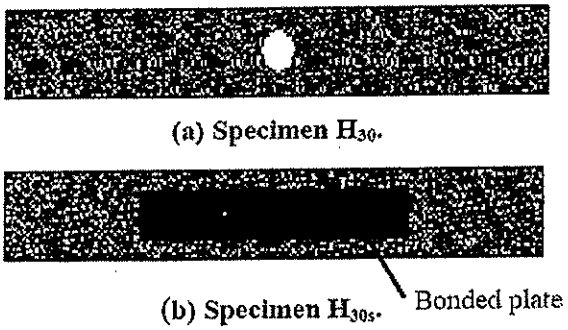

Fig.3. Configuration of connections H_{30} and H_{30s}

2.3 Materials

The adhesive used for bonding steel plates was two-part epoxy impregnation resin (Sika-dure 330) of 4500 MPa modulus of elasticity, 30 MPa tensile strength and 0.9% elongation at break. The properties of the steel plates were 240 MPa yield strength, 300 MPa ultimate strength, 210 GPa modulus of elasticity and 0.3 Poisson's ratio.

3. FINITE ELEMENT ANALYSIS

The general purpose finite element program ABAQUS was used [12]. The ABAQUS was selected to perform the numerical analysis due to its

powerful and comprehensive functions and precision, especially in nonlinear analysis including nonlinear material properties, nonlinear geometries and nonlinear responses. The von Misses yield criterion was adopted in the nonlinear analysis. The eight-node brick element (C3D8) was employed to model the steel plates, adhesive layer and CFRP plate. Different mesh sizes were used to test the convergence and to get the appropriate accuracy of numerical solution.

3.1. Boundary Conditions

All modeled specimens or connections were fixed supported in one side and tensioned from the other side. To achieve the previous boundary conditions, two plates were attached to both ends of the modeled specimens or connection to avoid SC. The load was applied in increments as static load. The modified standard/static general method was used. The automatic load control scheme was followed.

3.2. Materials Modeling

The smeared crack approach available in ABAQUS was invoked to model the epoxy in the adhesive layer. The model assumed that the direct stress across the crack gradually reduces to zero as the crack open. The reduction in shear modulus due to epoxy cracking was defined as a function of direct strain across the crack in the shear retention model. The shear retention model states that the shear stiffness of the opened cracks reduces linearly to zero as the crack opening increases. The stress-strain curve for epoxy is approximately linear elastic up to the maximum tensile strength of epoxy with maximum strain, ε_{max}, of 0.009. After this point, the epoxy cracked and its strength decreased gradually up to zero. The failure ratio option was used to define the failure surface of epoxy. The steel plates modeled as a classical elastic plastic material with strain hardening. A bilinear stress–strain relationship was used for steel plates.

4. RESULTS AND DISCUSSION

The three connections (D, E and H) were failed due to debonding of the steel plates. The load elongation curves for the three beams obtained experimentally and those obtained numerically are shown in Fig. 4. The three connections show similar stiffness. The failure loads measured experimentally for the three steel connections (D, E and H) are 46.5, 54, 43 kN respectively while those obtained numerically are respectively 47.5, 57.5 and 43.2. It is clear that, there is an agreement between the numerical and experimental results. It is found that, the change in the end configuration affects the failure loads of the three connections. The connection E with end tapered bonded plates recorded the highest ultimate load while the connection H of the bonded plate having curved ends showed the lowest ultimate load. The presence of tapered plate ends at the bonded plate ends of the joint reduces the bond SC at that location which prevented cracking of the adhesive and this confirm with Dawood and Rizkalla [13]. Forming the bonded plate ends as a curve reduced the bonded area between the main plate and the bonded plates and thus reduced the capacity of the connection. Photo 1 shows the fracture shape for connection H resulted from the experimental work. The crack pattern of connection D obtained from the numerical analysis is shown in Fig 5. This figure shows that, yielding started in the main plate at the two ends of the bonded plates. This is a combined with debonding initiation at these locations. This new debonding area is a favorable zone for the growth of yielding which is a combined by a development of another new debonding area. This sequence of debonding failure is observed in all tested connections. Therefore, it can be concluded that the growth of debonding failure associated with the yielding growth in the main plate.

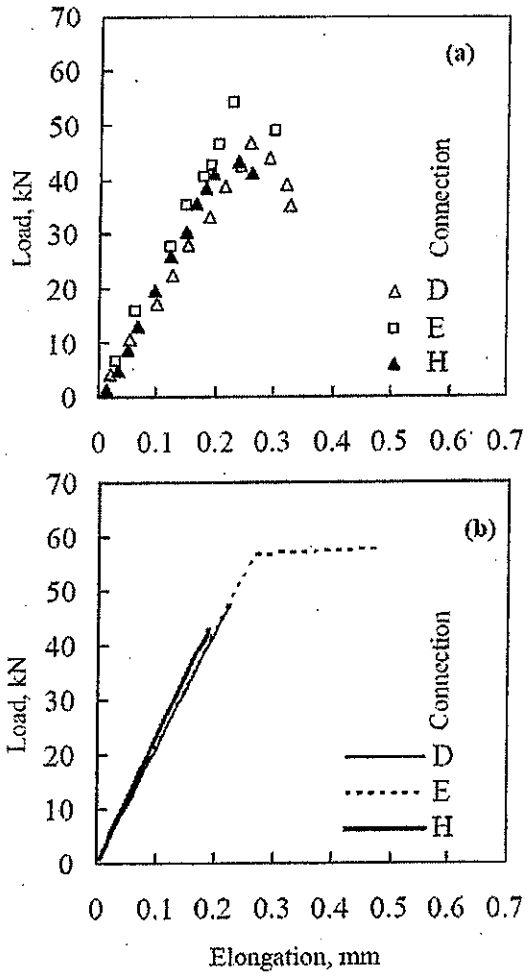

Fig. 4 Load elongation curves for connections D, E and H **(a)** Experimental **(b)** Numerical

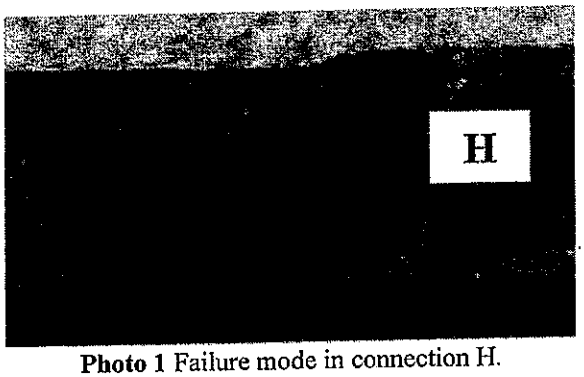

Photo 1 Failure mode in connection H.

This phenomenon will continue until removing the shielding around the sites of SC (i.e. DEN, CH, or main plate cutoff). Finally sudden failure occurred as shown in Photo.2. On the other hand, the ultimate load of the reference plate without connection measured experimentally was 72 kN, i.e. the ratio of the ultimate load of the best connection to that of the reference plate is equal to 0.75. This means that the efficiency of adhesive bonded joint in steel structures after yielding is very low.

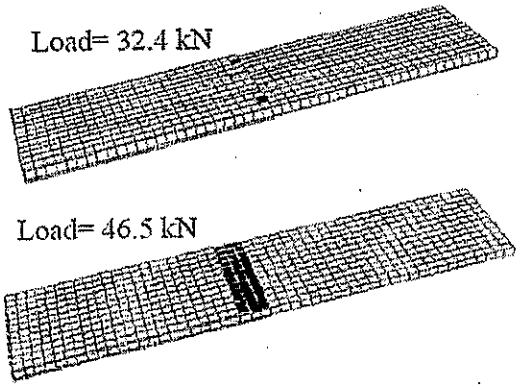

Fig 5 Crack pattern obtained for connection D.

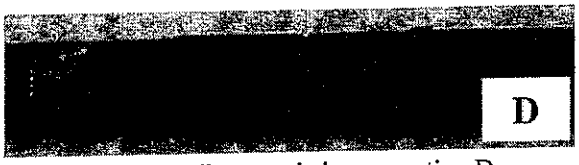

Photo 2 Failure mode in connection D.

The effect of the length of the bonded steel plates was studied in this group for the connection N. The experimentally recorded failure load for connection N was 51 kN while the numerical value was 56.4 kN. Comparing these results with those of connection D showed that, increasing the bonded plate length resulted in an increase in the capacity of the connection. The enhancement in the ultimate load with increasing the length of the bonded plates is some what small (≈11%) compared to doubling the length of the bonded plate. This can be attributed to the increase in the elongation with increasing the main plate length which accelerates the rate of debondiong failure. The comparison between the experimental and numerical load elongation curves for the two connections (D and N) is shown in Fig. 6. The figure shows that at certain applied load, the connection N recorded higher elongation than connection D, while, the ratio of the bonded plate length to that of the main plate length was constant and equal to 0.5. This is confirming with the basics, the elongation increases with the increase in the gage length, for the same cross section area and under tensile loads.

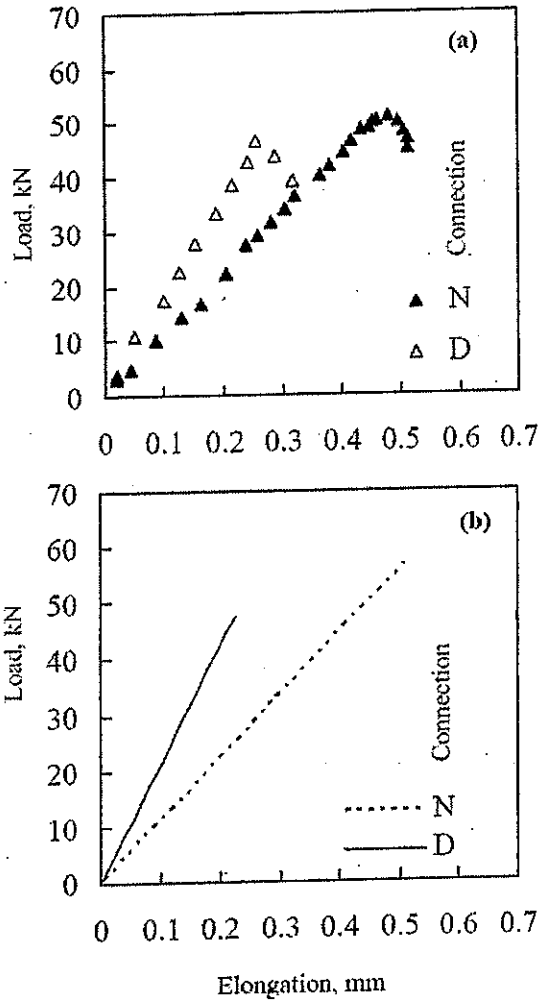

Fig. 6 Load elongation curves for connection D and N **(a)** Experimental **(b)** Numerical

For the second group, the three cracked connections A, B and C were failed due to debonding between the main plate and debonded plates followed by main plate cutoff. The experimentally and numerically obtained load elongation curves for the three beams are shown in Fig. 7. The load elongation curve for the un-strengthened plate (U) is also presented in the

figure. Similar stiffness for the three beams is observed. The failure loads measured experimentally for the three specimens are respectively 56, 52 and 51 kN, while that of plate U is 50.6. The ultimate loads increased with small extent as the bonded plate length increases from 200 mm to 250 mm but a marginal increase is observed on increasing l_{BP} from 150 to 200 mm. From the numerical results, changing the length of bonded steel plates for the two connections (A and B) had no pronounced effect on the ultimate load of the two specimens. On the other hand, the reduction in the bonded steel plate length reduced the ultimate load of specimen C. The shape of the three specimens after fracture is shown in photo 3. While the crack pattern obtained from the numerical analysis for specimen A is shown in Fig 8. The sequence and mode of failure of these connections are similar to that observed in lapped joint specimens, compare Figs. 5 and 8.

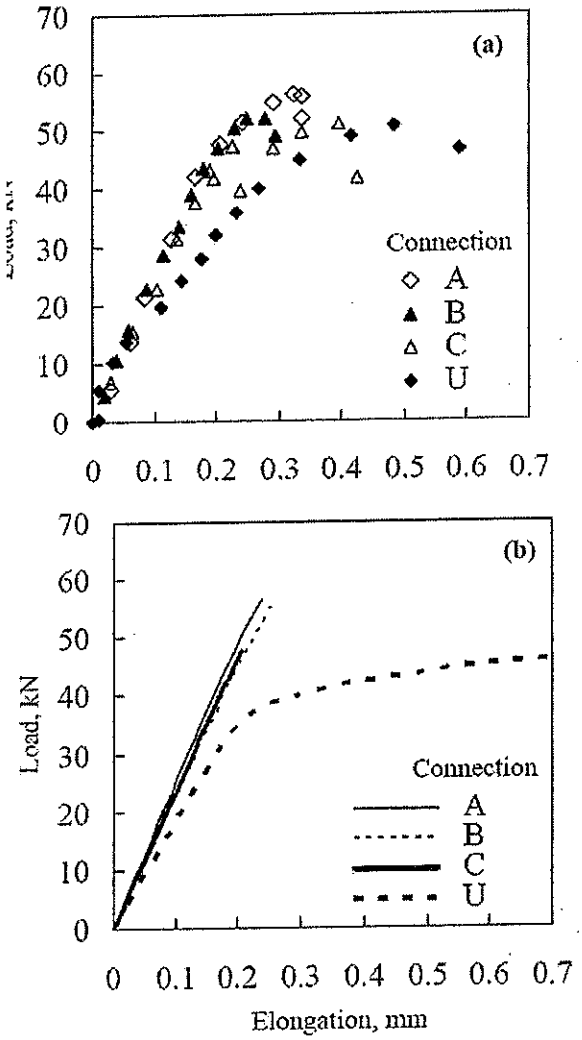

Fig. 7 Load elongation curves for connections A, B, C and U **(a)** Experimental **(b)** Numerical

The effect of CH in steel plates was studied in this group. The experimental and numerical results of the plate with CH and that shielded with two bonded covered plated 30 mm each is shown in Fig.9. The plate with a CH (H30) gave a max. load of 33.3 kN, while, this plate when shielded by two bonded plate of 30 mm width for each one (H30S) gave a max. load of 55 kN.

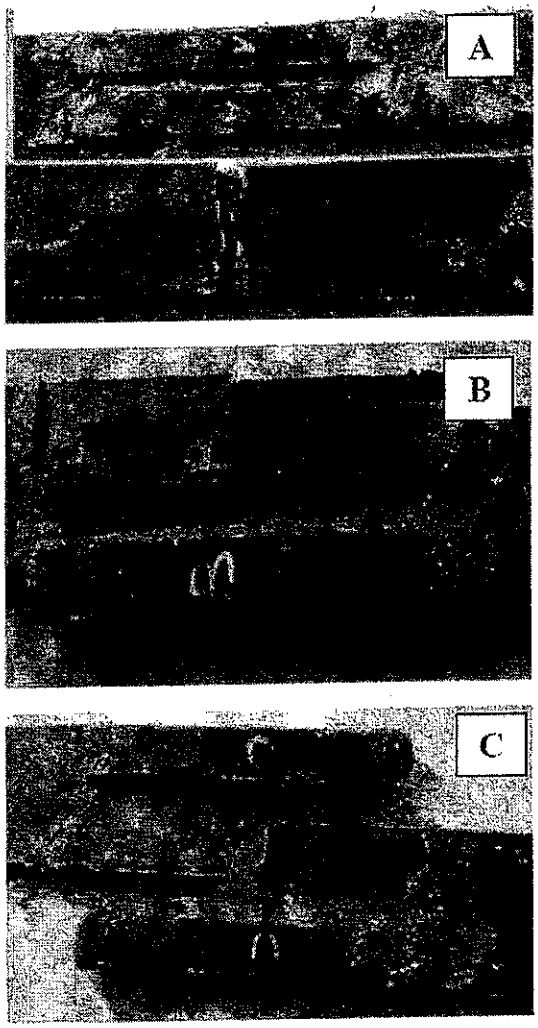

Photo 3 Failure mode in connections A, B and C.

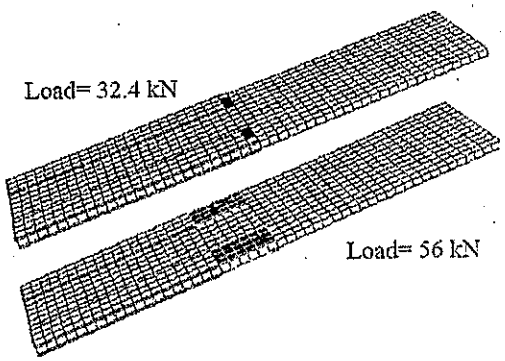

Fig 8 Crack pattern obtained for connection A.

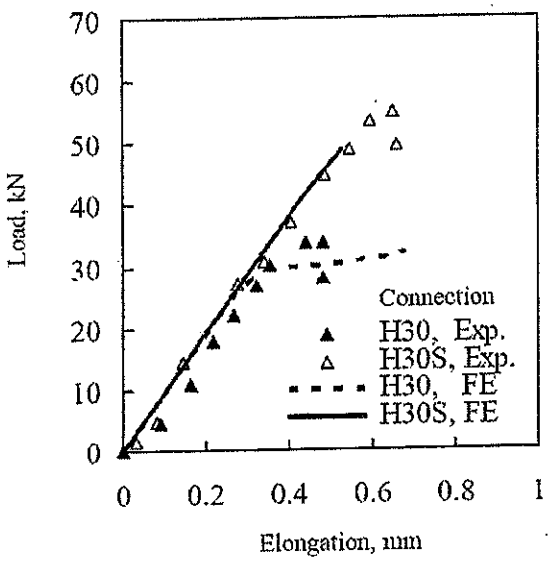

Fig. 9 Load elongation curves for connections H30 and H30S

Therefore, the bonded two cover plates are almost restore the strength of the plate with CH. This means that, the adhesive bonded plate has a high efficiency before the steel yielding. Photo 4 shows the mode of failure of such plates. This photo support the sequence of damage growth found in the cut-off, DEN, and CH connections.

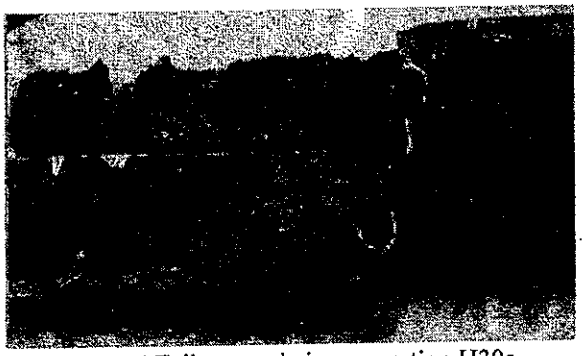

Photo 4 Failure mode in connection H30s.

Figure 10 shows the relation between the elastic stress concentration factor (SCF), K_t, of the damage (DEN and CH) shielded by two covering adhesive bonding plates, $K_{t\text{-}Sh}$, to that of the unshielded main plate, $K_{t\text{-}Ush}$, for the two cases. Large reduction in SCF is observed for the case of DEN compared to that of CH. Furthermore, $K_{t\text{-}Ush}$ of DEN, = 8.7, is about three time of that of CH, = 3, while, $K_{t\text{-}Sh}$ in both cases are lower than unity $\cong$ 0.95. This means that, the root of DEN is considered as another site of yielding or debonding initiation, see the development of cracks in Fig. 8. This may explain why the efficiency of covered plates failed to restore the plate with DEN similar to that with CH.

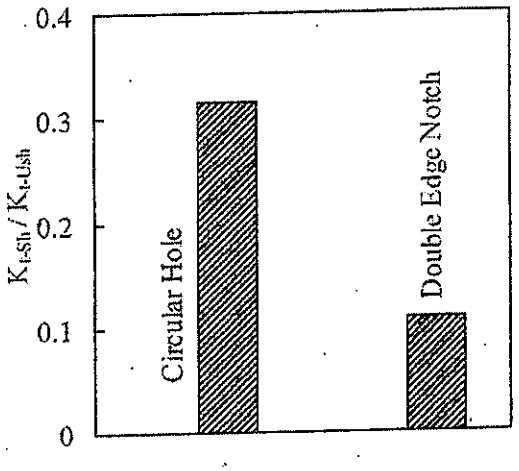

Fig 10 Effect of notch geometry on the K_t ratio.

5. CONCLUSIONS

Based on the present experimental and numerical results, the following conclusions may be drawn:

1- There is an agreement between the experimental and numerical results.

2- End tapered bonded plates recorded the highest ultimate load while the bonded plate having curved ends showed the lowest ultimate load.

3- For all tested connections, yielding always started in the main plate at the two ends of the bonded plates which is a combined with debonding initiation at these locations.

4- The bonded two cover plates are almost restore the strength of the plate with a circular hole.

5- Adhesive bonded plates diminished the elastic SCF of DEN and CH.

6. REFERENCES

[1] Xia, S.H. and. Teng, J.G, Behavior of FRP-to-Steel Bonded Joints, Proceedings of the International Symposium on Bond Behavior of FRP in Structures (BBFS 2005) Chen and Teng (eds)

[2] Luke, S., The use of carbon fiber plates for the strengthening of two metallic bridges of an historic nature in the UK, Proceedings of the international conference on FRP Composites in Civil Engineering, Hong Kong, 2001.

[3] Miller, T. C., Chajes, M. J., Mertz, D. R., and Hastings, J. N. Strengthening of a steel bridge girder using CFRP plates. Journal of Bridge Engineering, ASCE, Vol.6, No. 6, pp. 514-522, 2001.

[4] Stratford, T.J. and Chen, J.F., designing for tapers and defects in FRP-strengthened metallic structures, Proceedings of the International Symposium on Bond Behavior of FRP in Structures (BBFS 2005) Chen and Teng (eds)

[5] Al-Emrani M , Linghoff D. and Kliger R, bonding strength and fracture mechanisms in composite steel-CFRP elements, Proceedings of the International Symposium on Bond Behavior of FRP in Structures (BBFS 2005) Chen and Teng (eds)

[6] Tounsi, A., Hassaine Daouadji, T., Benyoucef, S., Addabedia, E. A., Interfacial stresses in FRP-plated RC beams: Effect of adherend shear deformations International Journal of Adhesion & Adhesives, Vol. 29, No. 4, pp343–351, 2009.

[7] Hollaway L. C, Cadei, J., Progress in the technique of upgrading metallic structures with advanced polymer composites. Prog Struct Eng Mater, Vol. 4, No. 2, pp 131–48, 2002.

[8.] Sallam, H.E.M., Saba, A.M., Mamdouh, W., Maaly, H. and Ibrahim, I., Strengthening of steel beams using bonded CFRP and steel plates: A pilot study, Al-Azhar Univ. Engng. Journal, Vol. 8, No. 10, pp. 23–29, (2005).

[9] Sallam, H. E. M., Ahmed, S. S. E., Badawy, A. A. M. and Mamdouh, W., Evaluation of steel I-beams strengthened by various plating methods, Advances in Structural Engineering, Vol. 9, No. 4, pp 535-544, 2006.

[10] Colombi, P., Poggi, C., An experimental, analytical and numerical study of the static behavior of steel beams reinforced by pultruded CFRP Strips, Composites: Part B, Vol. 37, No. 1, pp. 64–73, 2006.

[11] Deng, J., Marcus M. K. Lee, Effect of plate end and adhesive spew geometries on stresses in retrofitted beams bonded with a FRP plate, Composites: Part B, Vol. 39, No. 4, pp. 731–739, 2008.

[12] ABAQUS User's Manual, Version 6.3, Hibbitt, Karlsson and Sorensen, Inc., Pawtucket, R.I, 2002.

[13] Dawood, M. and Rizkalla, S., Bond and Splice Behavior of Cfrp Laminates for Strengthening Steel Beams, Accepted for Publication in the Proceedings of the International Conference on Advanced Composites in Construction (ACIC 07), University of Bath, Bath, United Kingdom, April 2-4, 2007.